International Journal of GEOMATE, Feb., 2019 Vol.16, Issue 54, pp.134- 139
Geotec., Const. Mat. & Env., DOI: https://doi.org/10.21660/2019.54.8230
ISSN: 2186-2982 (Print), 2186-2990 (Online), Japan

DISCRETE PARTICLE SIMULATION MODEL FOR SLAKING OF GEOMATERIALS INCLUDING SWELLING CLAY MINERALS

*Yutaka Fukumoto[1] and Satoru Ohtsuka[1]

[1]Department of Civil and Environmental Engineering, Nagaoka University of Technology, Japan

*Corresponding Author, Received: 10 Oct. 2018, Revised: 17 Nov. 2018, Accepted: 22 Dec. 2018

ABSTRACT: The slaking of geomaterials often causes some unexpected geohazards, such as slope failures, debris flows, rockfalls, and so on. In particular, the process of slaking is highly enhanced when the geomaterials include swelling clay minerals such as montmorillonite and saponite. In order to investigate the mechanisms of the slaking phenomenon from a microscopic point of view, this study presents a particle simulation model based on the discrete element method (DEM) that can reproduce the slaking process of geomaterials that include swelling clay minerals. The properties of swelling and shrinking are modeled by changing the diameter of the DEM particles which are assumed to comprise the swelling clay minerals and several sand particles. A series of simulations of the deformation of mudstone under a wet-dry cyclic condition is performed in both two and three dimensions. As a result of the analyses, the applicability of the proposed model to the slaking phenomenon is confirmed.

Keywords: Slaking, Swelling clay mineral, Mudstone, Discrete element model, Granular materials

1. INTRODUCTION

The slaking phenomenon is described as the process in which compacted soils or rocks gradually disintegrate into fine fractions under a wet-dry cyclic condition. The slaking of geomaterials often contributes to the risk of some geohazards, such as slope failures, debris flows, rockfalls, and so on [1]. In particular, when the geomaterials include swelling clay minerals, such as montmorillonite and saponite, which are classified in the smectite group, the slaking phenomenon is highly enhanced and the potential for geohazards increases considerably. Previous researches have revealed that many factors can trigger the slaking phenomenon [2], [3], but each factor has not yet been systematically defined.

In order to investigate the mechanisms of the slaking phenomenon from a microscopic point of view, this study presents a particle simulation model based on the discrete element method (DEM) that can reproduce the process of the slaking of geomaterials that include swelling clay minerals. In the model, the characteristics of swelling and shrinking are modeled by changing the diameter of the DEM particles which are assumed to comprise the clay minerals and several sand particles. In addition to this model, a model of cohesion is introduced to the contact logic between the DEM particles so that cohesive materials, such as compacted soils and rocks, can be reproduced in the framework of the DEM.

A series of simulations of the deformation of mudstone, subjected to cycles of wetting and drying, is performed in both two and three dimensions. As a result of the analyses, the applicability of the proposed model to the slaking phenomenon is confirmed.

The present paper is organized as follows. At the beginning of the paper, the numerical methods are firstly described. Details of the results of the numerical simulations and discussions are then given in the following sections. A summary and the limitations of the proposed numerical model are presented in the final section.

2. MODEL OF SWELLING AND SHRINKING

A numerical model which can simulate the characteristics of the swelling and shrinking of clay minerals is developed on the basis of the conventional DEM [4]. In the proposed model, the DEM particles are assumed to represent the area where several sand particles and clay minerals exist, as shown in Fig. 1, where the dotted circles indicate the DEM particles. When the soil contains water, the clay minerals swell and are pushed inside the pores of the sand particles; and thus, they enlarge the size of the DEM particles. When the soil is exposed to a dry condition, on the other hand, the clay minerals shrink; and thus, the size of the DEM particles also shrinks. Such a model, which deals with the changing size of DEM particles, is found in some literature [5], [6], where the patterns of the surface cracks of the clay soils are studied.

The initial diameter of DEM particles is defined as D_{ini} (m). In the following sentences, the direction of swelling is negative and that of shrinking is positive. The upper limit of the amount of swelling is defined as $-\alpha_{\mathrm{sw}}D_{\mathrm{ini}}$ (m), while the upper limit of

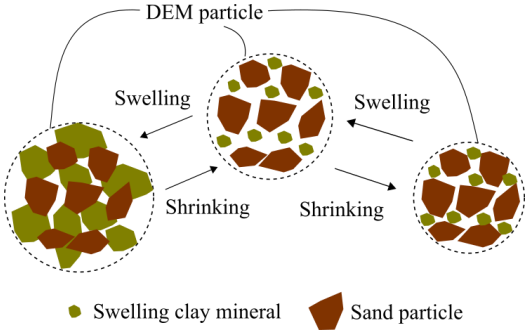

Fig. 1 Model of swelling and shrinking in the framework of DEM

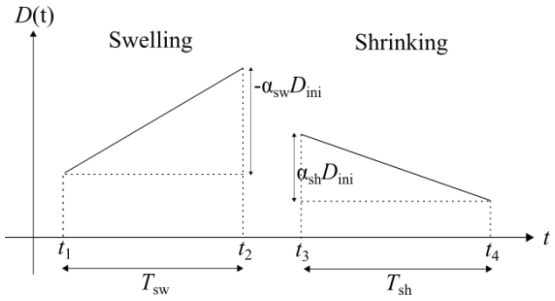

Fig. 2 Parameters for model of swelling and shrinking

the amount of shrinking is defined as $\alpha_{sh}D_{ini}$ (m), as shown in Fig. 2. It should be noted here that swelling coefficient α_{sw} is a negative value and that shrinking coefficient α_{sh} is a positive value. The values for α_{sw} and α_{sh} are non-dimensional. The variation in the diameter of each DEM particle against time is assumed to be linear for simplicity.

The times required to reach the limit value of the swelling and the shrinking are T_{sw} (s) and T_{sh} (s), respectively. When t_1 (s) is the starting time of the swelling, t_2 (s) is the ending time of the swelling, t_3 (s) is the starting time of the shrinking, and t_4 (s) is the ending time of the shrinking, the diameter of the DEM particles at t (s) is obtained as follows:

$$D(t) = D(t_1) - \frac{\alpha_{sw} D_{ini}}{T_{sw}}(t - t_1), t_1 < t < t_2, \quad (1)$$

$$D(t) = D(t_2) - \frac{\alpha_{sh} D_{ini}}{T_{sh}}(t - t_3), t_3 < t < t_4, \quad (2)$$

where t (s) is the time. The velocity of the swelling is $-\alpha_{sw}D_{ini}/\ T_{sw}$ (m/s) from Eq. (1) and the velocity of the shrinking is $-\alpha_{sh}D_{ini}/\ T_{sh}$ (m/s) from Eq. (2). From the viewpoint of computational costs, the values for T_{sw} (s) and T_{sh} (s) in the numerical simulations are set to be smaller than the actual scale of time.

In this model, the shape of $D(t)$ is linear and it is independent of the water content of the soils. A non-linear model for $D(t)$, which can consider the water content or the chemical reactions, is a topic for future study because the slaking phenomenon includes not only a mechanical process, but also a hydraulic process and a chemical process.

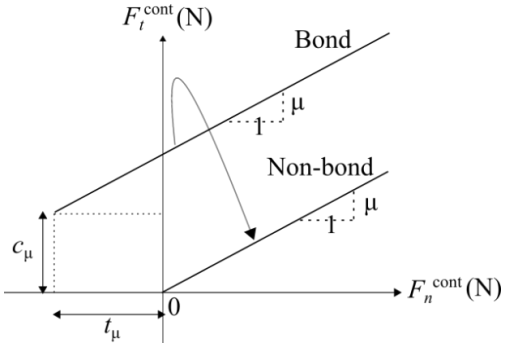

Fig. 3 Model of linear contact bond

3. MODEL OF COHESION

3.1 Contact Logic

In addition to the model of the swelling and shrinking, a model of the cohesion is introduced to the contact logic in order to express the compacted soils or rocks. The model of the cohesion is composed of two models, namely, the linear contact bond model and the rolling friction model. The total of the three input parameters is attached to the model of the cohesion.

The DEM permits the neighboring particles to be bonded together by springs which can transmit both attractive and repulsive forces. Among these bond models, the linear contact bond model [7], [8] requires only two micromechanical parameters for a transformation from the unbonded case to the bonded case. This bond model is characterized by the adaptation of the Mohr-Coulomb failure criterion into the F_n^{cont}–F_t^{cont} plane, as shown in Fig. 3, where F_n^{cont} (N) is the normal contact force and F_t^{cont} (N) is the tangential contact force. The values for the slope of the lines in Fig. 3 indicate the coefficient of sliding friction μ. The two kinds of input parameters are the contact bond force in the tangential direction, c_μ (N), and the contact bond force in the normal direction, t_μ (N).

Furthermore, in order to consider the effect of the inter-particle cohesion on the torque of the DEM particles, a rolling friction model [9] is also introduced. The rolling friction model employed in this study is the same as that employed in our previous research [9]. The moment of rolling resistance, resulting from the rolling friction, is defined as a function of the normal contact force, F_n^{cont} (N), and a length parameter to represent the contact area, b. Length parameter b is a ratio of the width of the virtual contact area to the diameter of

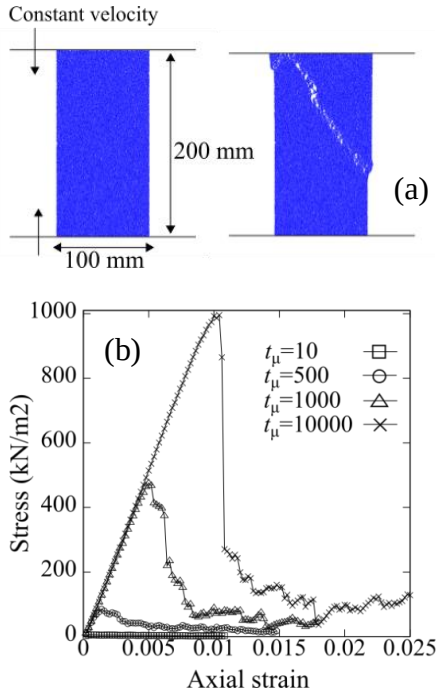

Fig. 4 Simulation of uniaxial compression test

the DEM particles, and it is the input parameter for the rolling friction model.

3.2 Uni-axial Compression Test

Two-dimensional simulations of the uniaxial compression test are performed, as illustrated in Fig. 4 (a), so that the correlations between the micromechanical parameter and the uniaxial compressive strength can be obtained. In the simulation, the upper wall and the lower wall are controlled with the same constant velocity in the direction of compression.

The specimen is 100 (mm) in width and 200 (mm) in height. The specimen consists of 23,397 DEM particles whose average diameter is 1 mm. The density of the circular DEM particles is 2600 (kg/m^2). The contact springs, for both the particle-particle contacts and the particle-wall contacts, are assumed to be linear. The value for k_n/ k_t = 4 (k_n (N/m) = 1.0×10^8 and k_t (N/m) = 2.5×10^7), where k_n and k_t are the normal and the tangential spring constants, respectively. In addition, viscous damping is introduced so that the equilibrium state can be achieved. The damping was constrained to be small enough so as not to have any effect on the results presented in this study. The value for the coefficient of the sliding friction is 0.5. The value for the rolling friction parameter is 0.1. The values for the contact bond force in the normal direction, t_μ (N), are set to be in the range of 10 to 10,000, while those for the contact bond force in the tangential direction, c_μ (N), are set to be 0.

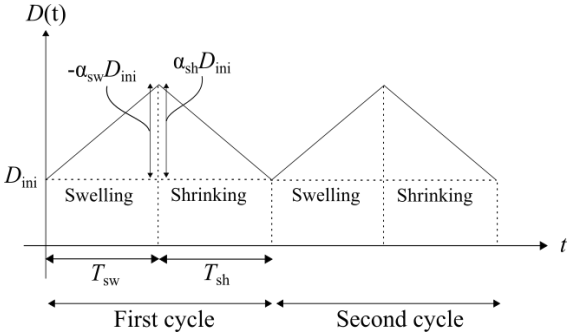

Fig. 5 Parameters for simulation of wet-dry cyclic condition

Figure 4 (b) plots the stress – strain curves obtained from the uniaxial compression test. The results of t_μ (N) = 10, 500, 1000, and 10000 are presented here. The maximum values for the compressive stress indicate the uniaxial compressive stress. It can be seen from the figure that the values for the obtained strength depend on the contact bond force and vary in the range of 0 to 1000 (kN/m^2). The model of the cohesion is appropriate for the purposes of the present research because the typical value for the uniaxial compressive stress of mudstone often varies in the range of 100 to 10000 (kN/m^2). It should be noted here that further investigations, such as a uniaxial tension test and a diametral compression test, in addition to the uniaxial compression test, are necessary for determining more detailed relationships between the micromechanical parameters and the micromechanical strength.

4. 2D SIMULATION OF SLAKING PHENOMENON

The numerical simulation of the slaking of mudstone under a wet-dry cyclic condition in two dimensions is performed in order to confirm the applicability of the proposed model. The initial size of the specimen at t (s) = 0 is 100 mm in width and 100 mm in height. The number of DEM particles which comprise the specimen is 12,998, and the average diameter of each DEM particle is 1 mm. The time step is 5.0×10^{-7} (s). The values for the normal and the tangential spring constants are 1.0×10^8 (N/m) and 2.5×10^7 (N/m), respectively. The values for μ and b are 0.5 and 0.1, respectively. The above numerical conditions are almost the same as those used in the uniaxial compression test.

In terms of the model of the swelling and shrinking, the input parameters are set as described in Fig. 5: $\alpha_{sw} = -0.1$, T_{sw} (s) = 2.0, α_{sh} = 0.1, and T_{sh} (s) = 2.0. The cycle of swelling and shrinking is repeated two times, i.e., the total time of the simulation is 8.0 s. In the first cycle, the shrinking

process is started immediately after the end of the swelling process. At the beginning of the second cycle, the swelling process is started immediately after the end of the shrinking process.

Figure 6 shows the snapshots of the cases of contact bond force, t_μ (N) = 10, 50, and 100, in which three different patterns of slaking are obtained. When the value for t_μ (N) is larger than 100, the specimen shows little change from the initial state. Neither deformations nor small cracks can be observed inside the specimens in such cases.

At first, Fig. 6 (a) shows the case of t_μ (N) = 10 where the contact bond is very small. From the illustrations, it can be seen that the specimen already begins to collapse at t (s) = 2.0 and largely collapses at t (s) = 8.0. With this pattern of the slaking phenomenon, the magnitude of the collapse is very large and the soil specimen cannot retain the original shape at the end of the second cycle.

Next, the case of t_μ (N) = 50 is presented in Fig. 6 (b). Based on the snapshots, there are neither cracks nor deformations inside the specimen at the end of the first cycle. However, at the end of the second cycle, it can be seen that the specimen has changed a little in shape. From the enlarged drawing at t (s) = 8.0, which is illustrated in Fig. 7 (a), there are some voids inside the specimen, i.e., cracks are generated. In the second pattern of the slaking phenomenon, the soil specimen deforms to a small extent and a lot of cracks appear at the final state.

Finally, Fig. 6 (c) shows the case of t_μ (N) = 100. In this case, the shape of the specimen remains square at the end of the second cycle. From Fig. 7 (b), it can also be observed that there are no cracks or deformations. When the value for t_μ (N) is larger than 100, the specimen shows the same trends as the case of t_μ (N) = 100. In the third pattern of the slaking phenomenon, the soil specimen retains the original shape, even though it is subjected to two cycles of wetting and drying.

In order to discuss these changes in the mudstone in detail, the evolution of the number of bonded contacts between the DEM particles is presented in Fig. 8 (a). For all cases, in the first cycle of the wet-dry condition, a lot of the bonded contacts are broken in the swelling process in comparison to the shrinking process. In particular, in the cases of t_μ (N) = 10, the same trends are also obtained in the second cycle. However, in the cases of t_μ (N) = 50 and 100, the variation in bonded contacts has a different tendency from that in the first cycle. From Fig. 8 (b), which is the extended view of Fig. 8 (a) in the second cycle, the decrease in bonded contacts in the shrinking process is larger than that in the swelling process. It is believed that the microscopic mechanisms of slaking at a particle

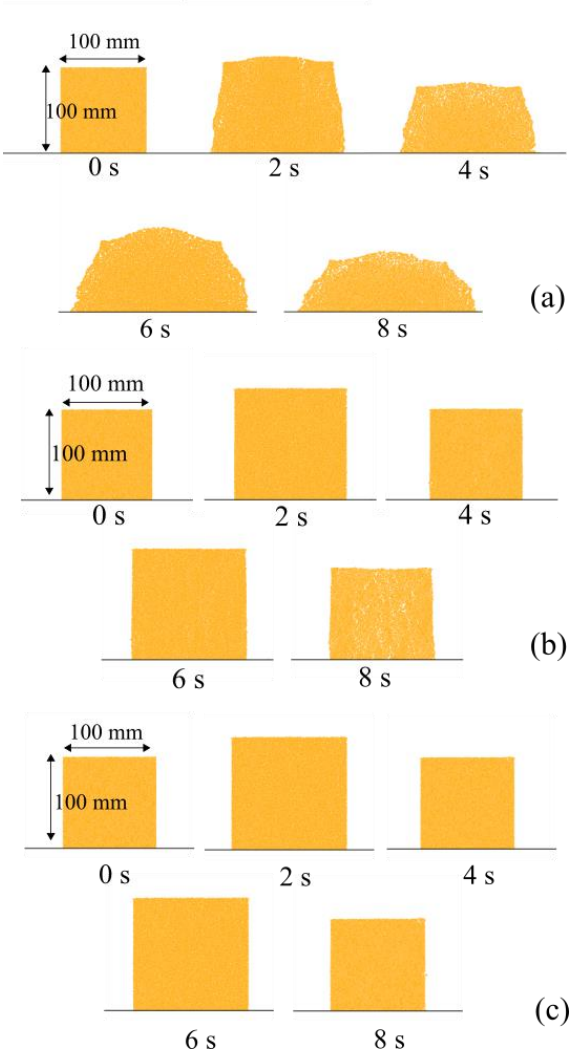

Fig. 6 Snapshots of simulation: (a) t_μ (N) = 10. (b) t_μ (N) = 50. (c) t_μ (N) = 100

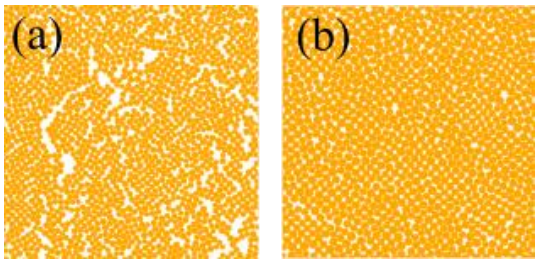

Fig. 7 Enlarged illustrations at t(s) = 8.0: (a) t_μ (N) = 50 (b) t_μ (N) = 100. Magnification ratio of the figure is about 20

resolution may also be different from the patterns of the macroscopic deformations.

As stated in the above discussions, the presented simple numerical model can obtain three types of slaking behavior of the mudstone that depend on the parameters of the contact bond. However, the

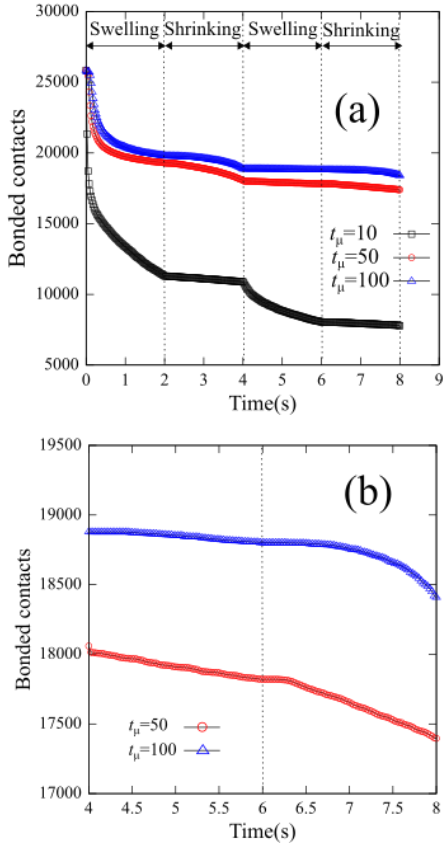

Fig. 8 (a) Time evolution of bonded contacts (b) Extended view of time evolution of bonded contacts in second cycle

numerical conditions of t_μ (N) = 10, 50, and 100 do not correspond to the actual uniaxial compression strength of mudstone, as discussed in the previous section. To solve this problem, a model of the cohesion which varies according to the water content is needed in the future.

5. 3D SIMULATION OF SLAKING PHENOMENON

In addition to the investigation in two dimensions, the results of the three-dimensional simulation are discussed briefly in order to validate the applicability of the proposed model in the 3-D condition. The simulation demonstrates the deformation of a cylindrical sample of mudstone taken by a boring exploration in a core box, as shown in Fig. 9. The mudstone sample includes swelling clay minerals and is subjected to wetting and drying in the same manner as the investigation in the 2-D condition.

At the initial state, the diameter of the specimen is 50 (mm) and the length of it is 320 (mm). The interior of the core box has the same length. The number of DEM particles which comprises the specimen is about one hundred thousand, and the average diameter of each DEM particle is 2 (mm). The time step is 2.0×10^{-7} (s). The values for the normal and the tangential spring constants are 1.0×10^{7} (N/m) and 2.5×10^{6} (N/m), respectively. The values for μ, b, t_μ (N), and c_μ (N) are set to be 0.5, 0.1, 100, and 50, respectively.

The parameters for the model of the swelling and shrinking are listed below: $\alpha_{sw} = -0.1$, T_{sw} (s) = 1.0, α_{sh} = 0.1, and T_{sh} (s) = 1.0. The cycle of swelling and shrinking is repeated only one time. The total time of the simulation is 2.0 (s). The shrinking process is started immediately after the end of the swelling process. This calculation is performed on a graphic processing unit. The parallelized algorithm for the DEM [10] is incorporated into our in-house code.

Figure 9 shows snapshots of the results of the numerical simulation. In the figure, the specimen positioned in the back shows the initial state at t (s) = 0 and that in the front shows the final state at t (s) = 2.0. It can be found that the left part of the specimen largely deforms. This is because shear stress acts on the specimen due to the restriction of the fixed side boundaries in the swelling process. In fact, such a deformation pattern can be observed in the actual soil sample taken by a boring exploration. On the other hand, a linear crack is generated on the surface of the lateral side of the cylinder. Several layered cracks are also observed in the actual soil sample, but this investigation cannot reproduce them.

6. SUMMARY

This paper has presented a simple discrete particle simulation model for the slaking phenomenon of geomaterials that include swelling clay minerals. In the investigation in two dimensions, three types of slaking behaviors of mudstone, that depend on the parameters of the contact bond, were successfully obtained. In the investigation in three dimensions, it was demonstrated that there are future prospects in the application of the model to 3-D problems. In a future study, it will be necessary for both the model of the swelling and shrinking and the model of cohesion to consider the effect of the water content and the chemical reaction. It will also be important to develop a detailed method to determine the input parameters from the results of laboratory experiments.

7. ACKNOWLEDGEMENTS

This work was supported by research funding from the Niigata Construction Technology Center.

Fig. 9 Simulation of deformation of cylindrical sample of mudstone taken by boring exploration in core box. Magnification ratio of the figure is 1.0

8. REFERENCES

[1] Kiyota, T., Sattar, A., Konagai, K., Kazmi, Z. A., Okuno, D., and Ikeda, T., Breaching failure of a huge landslide dam formed by the 2005 Kashmir earthquake. Soils and Foundations, Vol. 51, Issue 6, 2011, pp. 1179-1190.

[2] Kikumoto, M., Putra, A. D., and Fukuda, T., Slaking and deformation behaviour. Géotechnique, Vol. 66, Issue 9, 2016, pp. 771-785.

[3] Chigira, M., and Oyama, T., Mechanism and effect of chemical weathering of sedimentary rocks. Engineering Geology, Vol. 55, Issue 1-2, 2000, pp. 3-14.

[4] Cundall, P.A. and Strack, O.D.L., A discrete numerical model for granular assemblies. Géotechnique, Vol. 29, Issue 1, 1979, pp. 47-65.

[5] Péron, H., Delenne, J. Y., Laloui, L., and El Youssoufi, M. S., Discrete element modelling of drying shrinkage and cracking of soils. Computers and Geotechnics, Vol. 36, Issue 1-2, 2009, pp. 61-69.

[6] El Youssoufi, M. S., Delenne, J. Y., and Radjai, F., Self-stresses and crack formation by particle swelling in cohesive granular media. Physical Review E, Vol. 71, Issue 5, 2005, 051307.

[7] Utili, S., and Nova, R., DEM analysis of bonded granular geomaterials. International Journal for Numerical and Analytical Methods in Geomechanics, Vol. 32, Issue 17, 2008, pp. 1997-2031.

[8] Fukumoto, Y., Particle Based Multiphysics Simulation for Applications to Design of Soil Structures and Micromechanics of Granular Geomaterials, Ph. D thesis of Kyoto Univ., 2015.

[9] Fukumoto, Y., Sakaguchi, H., and Murakami, A., The role of rolling friction in granular packing. Granular Matter, Vol. 15, Issue 2, 2013, pp. 175-182.

[10] Nishiura, D., and Sakaguchi, H., Parallel-vector algorithms for particle simulations on shared-memory multiprocessors. Journal of Computational Physics, Vol. 230, Issue 5, 2011, pp. 1923-1938.